JOURNAL OF SYNCHROTRON RADIATION

ISSN: 1600-5775
journals.iucr.org/s

Rigorous calculations and synchrotron radiation measurements of diffraction efficiencies for tender X-ray lamellar gratings: conical *versus* classical diffraction

Leonid Goray, Werner Jark and Diane Eichert

J. Synchrotron Rad. (2018). **25**, 1683–1693

JOURNAL OF SYNCHROTRON RADIATION
ISSN 1600-5775

Rigorous calculations and synchrotron radiation measurements of diffraction efficiencies for tender X-ray lamellar gratings: conical *versus* classical diffraction

Leonid Goray,[a,b,c]* Werner Jark[d]* and Diane Eichert[d]

[a]Saint Petersburg Academic University, Khlopin St. 8/3 Let. A, St Petersburg 194021, Russian Federation, [b]ITMO University, Kronverkskiy Pr. 49, St Petersburg 197101, Russian Federation, [c]Institute for Analytical Instrumentation, RAS, Rizhsky Pr. 26, St. Petersburg 190103, Russian Federation, and [d]Elettra – Sincrotrone Trieste SCpA, SS 14 – km 163.5 in AREA Science Park, Basovizza, Trieste 34149, Italy.
*Correspondence e-mail: lig@pcgrate.com, jark@elettra.eu

Received 10 May 2018
Accepted 3 September 2018

Edited by P. A. Pianetta, SLAC National Accelerator Laboratory, USA

Keywords: diffraction gratings; diffraction theory; computational electromagnetic methods; X-ray optics.

When reflection gratings are operated at grazing incidence in the extreme off-plane configuration and the incident beam trajectory is parallel to the grooves, the diffraction into the first order can be more efficient than in the classical orientation. This situation is referred to as the conical diffraction case. In the classical configuration the grooves are perpendicular to the incident beam and thus an efficiency-reducing shadowing effect will be observed at very grazing angles. It was recently shown that a laminar grating could provide symmetric and relatively high efficiencies in conical diffraction for diffraction even of photons with large energies of the order of 4 and 6 keV. For photon energies in the tender X-ray range, accurate computing tools for the calculation of diffraction efficiencies from gratings with simple coatings have not been available. Promising results for this spectral range now require the development of tools for modelling the diffraction efficiency expected in optical instrumentation, in which the provision of high efficiency in the indicated spectral range is mandatory. This is the case when weak sources are to be investigated, like in space science. In this study it will be shown that scalar calculations are not appropriate for this purpose, while newly introduced rigorous calculations based on the boundary integral equation method, implemented in the *PCGrate*® code, can provide predictions that are in agreement with observed diffraction efficiencies. The agreement is achieved by modelling the exact surface profile. This applies for both the conical diffraction configuration and for the classical in-plane configuration, in which a significantly lower efficiency was obtained. Even though the profile of the presented grating was not perfect, but significantly distorted, the calculations show that efficiency-wise the structure provided already more than 75% of the ideally expected efficiency for conical diffraction. This is a very promising result for further optimization of diffraction gratings for use in the tender X-ray range.

1. Introduction

The soft X-ray range was defined by Attwood (1999) to cover those photon energies in the X-ray range that cannot be used for radiography experiments due to their very limited penetration range; this photon energy range extends from 300 eV to 8000 eV (or, in terms of wavelength λ, from 4.1 nm to 0.15 nm; wavelength λ and photon energy E are related *via* the simple formula $\lambda E = 1239.852$ nm^{-1} eV^{-1}). Within this region the photon energy range 2 keV < E < 8 keV is referred to as the tender X-ray range by Attwood (1999), as the X-rays are monochromated like harder X-rays by the use of bulk structures, *i.e.* periodic crystal structures (see, for example,

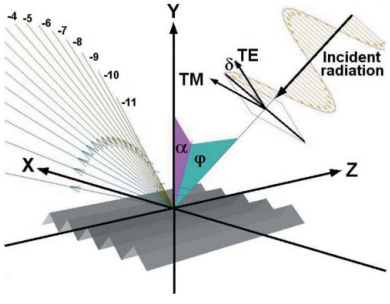

Matsushita & Hashizume, 1983). Lower photon energies instead are usually monochromated by surface relief structures, *i.e.* by reflection gratings (see, for example, Hutley, 1982).

Reflection gratings were classically found to be the most flexible devices for the monochromatization of visible and UV light (see, for example, Hutley, 1982). This is due to the fact that all important parameters, like the groove density, the grating orientation with respect to the incident beam and the angle of incidence, can be freely chosen. This situation changes significantly when the application range is extended towards soft X-rays as, according to Lukirskii *et al.* (1963), one now needs to operate the structure at grazing angles of incidence below the critical angle for total reflection θ_{crit}. When using a diffraction grating in the classical in-plane orientation, then the direction of the mth diffraction order for a given wavelength λ can be obtained from the grating equation,

$$m\lambda = p(\cos\theta - \cos\phi), \tag{1}$$

where p is the pitch (*i.e.* period or the groove spacing) of the structures in the plane of incidence (see Fig. 1), and θ and ϕ are the angles of grazing incidence and exit. m is positive for diffracted orders that are found between the incident beam and the direction of the specularly reflected beam. Then, in order to achieve monochromatization for $m \neq 0$, the angles θ and ϕ need to be different (see, for example, Hutley, 1982). Depending on the grating profile, parts of the incident and exiting beams will be subject to 'shadowing' effects, as discussed by Lukirskii *et al.* (1963), which are illustrated in Fig. 1. The areas shown in black are either not illuminated by the incident beam or they cannot diffract intensity into the exit direction. Then, either a fraction of the incident power can no longer leave the grating structure, *e.g.* from grooves of rectangular shape as shown in the lower part of Fig. 1, or a part of the structure cannot be the source of the exiting waves, as

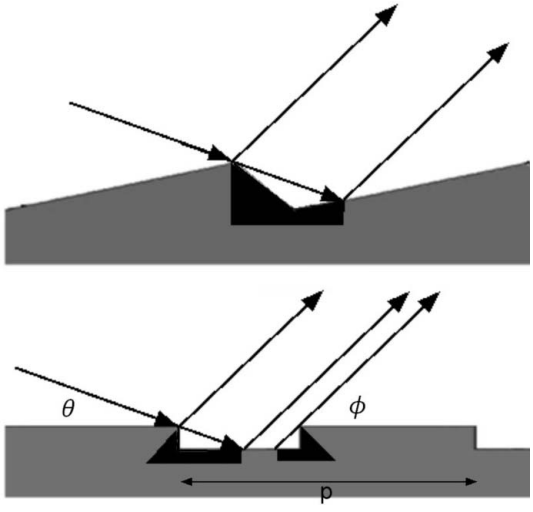

Figure 1
Sketch of the shadowing when diffraction gratings with sawtooth (top) and laminar profile (bottom) are operated at grazing incidence. p refers to the groove spacing, while θ and ϕ are the angles of grazing incidence and exit. The black areas are not illuminated or are not contributing intensity to the exiting beam, while the grey areas will diffract properly.

will be observed in the case of sawtooth (triangular) profiles (upper part of Fig. 1). Both effects will lead to discontinuities in the wavefront shape of the diffracted beam. Intuitively one would assume that the sawtooth profile (top of Fig. 1) could direct all incident power into only a single diffraction peak, which would be in the direction corresponding to specular reflection at the inclined groove surface. However, the reciprocity theorem requires that the efficiency of the diffraction is the same for a given deflection angle ($\theta + \phi$) also in the reversed trajectory (Maystre & Petit, 1976). The loss of photons in the shadow areas painted black is thus responsible for the reduction of the first-order efficiency. It was shown using rigorous calculations by Maystre & Petit (1976) and confirmed in experiments by Maystre *et al.* (1980) that the related diffraction efficiency for a given deflection angle can be predicted simply as the reflectivity of the grating coating material multiplied by the ratio of the unobstructed areas and the total area, as proposed by Lukirskii *et al.* (1963). For a sawtooth groove profile the latter ratio is the minimum of the ratios $\sin\theta/\sin\phi$ and $\sin\phi/\sin\theta$ as derived by Maystre & Petit (1976). For a given grating structure this ratio decreases with increasing photon energy, and for tender X-rays can be of the order of just a few percent or even smaller. This results in very small efficiencies for in-plane diffraction into a given order even though the reflectivity will be high. For this reason, in the few reported cases for gratings with simple coatings (*e.g.* Petersen, 1986), the transmission through grating monochromators was found to fall off rapidly in the tender X-ray range to an unusable level of mostly scattered light.

Greig & Ferguson (1950) were the first to point out that the shadowing can be avoided in sawtooth gratings when the incident beam trajectory is parallel to the grating grooves. This applies also to laminar grating profiles. In this orientation the intensity is diffracted off-plane, *i.e.* out of the plane of incidence, into a cone, the centre axis of which coincides with the intersection line between the plane of incidence and the grating surface. This advantageous situation is described either as the extreme off-plane configuration or as the conical diffraction scheme, in which the incident beam observes a periodic system of small parallel micro-mirrors. Relatively large efficiencies in this configuration have already been observed for softer X-rays with photon energies from about 300 eV up to 1500 eV by Werner (1977) and Cash & Kohnert (1982). This permits the use of such objects in space science instrumentation, which needs very efficient monochromatization schemes as the sources are very weak. The use of higher photon energies was not reported until very recently when efficient conical diffraction was observed by Jark & Eichert (2015, 2016) also for tender X-rays with photon energies >4 keV. At this point then the need exists to be able to predict the grating performance reliably in the previously unexplored tender X-ray range, where very small angles of grazing incidence will have to be used according to Lukirskii *et al.* (1963). For meaningful predictions the simulation of a real grating profile, which may be distorted compared with the ideal one, has to be possible. A solution to this theoretical problem will be discussed here; then it is investigated whether

for efficient diffraction the grating parameters can still be chosen freely.

This report now deals only with the efficient use of reflection gratings with simple coatings in the tender X-ray range. Thus it needs to be mentioned that, recently, promising developments were made for enhancing the previously observed low diffraction efficiencies of simple reflection gratings for photon energies above 2000 eV by the addition of appropriate multilayer coatings, for example by McNulty *et al.* (1997), Ishino *et al.* (2006), Choueikani *et al.* (2014) and Senf *et al.* (2016). In this case the shadowing effect in the classical orientation is overcome by the 'transparency' of the multilayer coating. The related high diffraction efficiencies also for fine-pitch gratings (Voronov *et al.*, 2015, 2016) can be reliably calculated theoretically (Gorai, 2005; Goray & Egorov, 2016). It goes beyond the scope of the present study to discuss more details of this approach.

2. Prediction of grating diffraction efficiency

2.1. Limitation due to the critical angle operation

We will consider the two extreme geometrical orientations of the grating with respect to the incident beam, *i.e.* the case of classical in-plane operation and the case of conical diffraction. The angular positions of the diffraction orders for the first case are given by equation (1). In combination with grazing incidence both angles θ and ϕ will be small and the cosine function in equation (1) can be developed into a series expansion, so that (1) can be written in the form

$$\frac{2m\lambda}{p} = \theta^2 - \phi^2 = (\theta + \phi)(\theta - \phi). \tag{2}$$

The validity of the reciprocity theorem and the requirement to operate any optical component efficiently with grazing angles below $\theta_{\rm crit}$ will now establish limiting values for the sum and the difference of the angles on the right-hand side of (2). This limit will here be referred to as the 'critical angle operation'. In an asymmetric profile, like a triangular or sawtooth profile, the angle of grazing incidence with respect to the inclined groove surface must stay below the critical angle for total reflection; this is also required for the case of the exiting beam. Consequently, the requirement for efficient diffraction is that the deflection angle $(\theta + \phi)$ into a given order needs to be smaller than $2\theta_{\rm crit}$. For a laminar profile the reciprocity theorem requests that both the angle of grazing incidence θ and the diffraction angle ϕ are smaller than the critical angle. For monochromatization they need to be different. Then for a laminar grating both terms on the right-hand side of (2) can at most be identical with the critical angle $\theta_{\rm crit}$. For a sawtooth profile the sum term can be twice as large.

Away from absorption edges of a material with the refractive index n the critical angle is defined by

$$\theta_{\rm crit} = \left[2(1-n)\right]^{1/2}, \tag{3}$$

when only the real part of the refractive index is considered. In this condition in the soft X-ray range the refractive index decrement $(1 - n)$ is a positive number which, according to James (1967), is given by

$$(1-n) = \frac{N_{\rm A}}{2\pi} r_0 \lambda^2 \rho \frac{Z}{A}, \tag{4}$$

where $N_{\rm A}$ is Avogadro's number, r_0 is the classical electron radius, ρ is the material density, λ is the photon wavelength, and Z and A are the atomic number and the atomic mass of the material, respectively. Then, from (3) and (4), one finds that the critical angle varies linearly with the photon wavelength with

$$\theta_{\rm crit} = a\lambda, \tag{5}$$

where $a = 64$ mrad nm^{-1} for the commonly used gold coating [for Pt it is $\sim$0.072 nm^{-1} (see Henke *et al.* (1993)]. For the desirable use of the grating away from the critical angle operation we then obtain from equation (2) a limit for the period for a laminar profile of

$$p_{\rm min,lam} > \frac{2}{a^2\lambda}|m|, \tag{6}$$

while for a sawtooth profile it is

$$p_{\rm min,saw} > \frac{1}{a^2\lambda}|m|. \tag{7}$$

With $1/a^2 = 244$ nm^2 for Au we have

$$p_{\rm min,lam} > \left(488\ {\rm nm}^2\right)\frac{|m|}{\lambda} \tag{8}$$

and

$$p_{\rm min,saw} > \left(244\ {\rm nm}^2\right)\frac{|m|}{\lambda}. \tag{9}$$

Now on the one hand, in order to minimize the obtainable spectral resolution, one has to strive for small groove spacing; and, technically, periods as small as $\sim$280 nm (groove density $\simeq 3600$ mm^{-1}) are now feasible with good shape fidelity. On the other hand, for efficient diffraction of high-energy tender X-rays with $E = 8$ keV ($\lambda = 0.15$ nm), equations (8) and (9) require gratings with $p_{\rm min,lam} > 3250$ nm (groove density < 300 mm^{-1}) and $p_{\rm min,saw} > 1625$ nm (groove density < 600 mm^{-1}). It is thus the combination of the critical angle operation and of the shadowing effect in higher groove density gratings which leads to the rapidly decaying monochromator transmission, when the photon energy of 2 keV is approached (*e.g.* Petersen, 1986). This latter photon energy coincides with the critical angle limit for a grating with $p = 820$ nm (1220 mm^{-1}), which will be discussed here. Conequently the operation range of similar high-groove-density gratings cannot be extended any further into the tender X-ray range. However, the situation changes completely when the grating is operated in conical diffraction. Then the direction of the mth diffraction order of a given wavelength λ can be obtained from the general grating equation, when expressed for conical diffraction, in the form given by Werner (1977),

$$-m\lambda/\sin\gamma = p(\sin\alpha - \sin\beta), \tag{10}$$

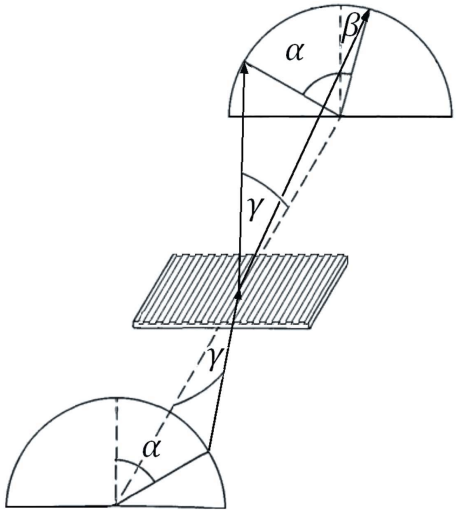

Figure 2
Schematic of conical diffraction. The angles α and β are the polar angles of incidence onto the surface and of diffraction, and γ is the azimuthal grazing incidence angle.

where α and β are the polar angles of incidence onto the surface and of diffraction, respectively, and γ is the azimuthal grazing incidence angle (the grazing angle of a rotation of the dispersive plane; see Fig. 2).

Assuming the incidence polar angle α to be zero (for symmetrical profiles) or to be small (for blaze profiles) and $\sin\beta \simeq 1$ for fine-pitch gratings working in conical grazing-incidence diffraction for the first orders, one can derive

$$\frac{m\lambda}{\gamma} \simeq p. \tag{11}$$

Using (3) for the expression of γ near the critical angle one obtains finally

$$p_{\min} > \frac{|m|}{a}. \tag{12}$$

Contrary to schemes of classical diffraction, equation (12) is valid for any groove profile and does not depend on the wavelength. In fact, for first-order diffraction by use of gold-coated gratings, equation (12) puts a limit on the very small number $p_{\min} > 15.6$ nm, which is achieved in all practical cases. It is worth noting that these rather rough evaluations for minimal periods are just the scalar theory conclusions and they must be verified against rigorous electromagnetic theory evaluations.

2.2. Scalar efficiency behaviour

An important feature in X-ray gratings is the small λ/p and h/p ratios, where h is the groove depth. The grating operates in the scalar regime if $\lambda/p < 0.2$ at $h/p < 0.1$ and the angles of incidence and diffraction are close to the surface normal. This is the situation discussed in text books (*e.g.* Born & Wolf, 1980). The scalar regime is characterized by the absence of polarization effects and anomalies, and the efficiency of perfectly reflecting (conducting) gratings can be determined from the universal curves plotted for various groove profile types by Maystre & Petit (1976). These curves are unique functions of the ratio h/p only and valid for gratings with various periods, depths and coating materials. Then in classical in-plane diffraction the absolute efficiency increases when the period increases. However, the observed variation of the efficiency with variation of the groove density is different from the expectations, as extrapolated from scalar theory, which postulates that the product of resolution with luminosity is constant. The efficiency η limits derived from the scalar diffraction theory for perfectly conductive gratings according to Born & Wolf (1980) are the following,

$$\begin{aligned} \eta &= 40.4\% \qquad \text{for laminar,} \\ \eta &= 100\% \qquad \text{for sawtooth.} \end{aligned} \tag{13}$$

The fundamental limitation in the use of the scalar approach for the calculation of the efficiency of bulk and multilayer gratings is given by the requirement that the incidence angle not be very grazing. According to Vidal *et al.* (1985) the angle of incidence with respect to the surface normal should not exceed 40° for bulk gratings and 45° for multilayer ones. Under grazing incidence at $\lambda/p < 0.1 \ldots 0.05$ the scalar approximation and even the rigorous perfectly conducting theory are generally unacceptable, especially for shorter periods, for the transverse magnetic (TM) polarization and for high orders. Gorai (2005) has already demonstrated by different rigorous calculations based on the differential, boundary integral equation, modal and Fourier-modal (coupled-wave) methods that the absolute efficiency of bulk and multilayer X-ray gratings changes unpredictably when compared with predictions based on the scalar theory even at very low λ/p, as the period, groove profile, incidence angle, wavelength and coating material vary. Only the optimum depths of standard groove profiles, which correspond to a blaze wavelength, can be predicted with an accuracy of a few dozens of percent as shown by Neviere & Flamand (1980). For classical diffraction,

$$\begin{aligned} |m|\lambda_{\text{blaze}} &= 4h\cos(D/2), \qquad \text{for laminar,} \\ |m|\lambda_{\text{blaze}} &= 2h\cos(D/2), \qquad \text{for sawtooth,} \end{aligned} \tag{14}$$

where D is the deviation angle between the incident and the diffracted beams. Now for grazing-incidence conical diffraction $D/2$ is not close to $\pi/2$ but can be rather small, like in near-normal-incidence classical diffraction. The conical type of diffraction is characterized by high luminosity when the angle of grazing incidence along the grooves is smaller than or equal to the critical angle. So, equations (14) are valid if we change $D/2$ to the incidence angle near the critical angle of the total external reflection. Then, equation (14) can be reformulated for conical diffraction mounts according to Vincent *et al.* (1979) as

$$\begin{aligned} |m|\lambda_{\text{blaze}} &= 4h\sin\gamma, \qquad \text{for laminar,} \\ |m|\lambda_{\text{blaze}} &= 2h\sin\gamma, \qquad \text{for sawtooth.} \end{aligned} \tag{15}$$

It is worth noting that equation (15), contrary to equation (14), does not include polar incidence and diffraction angles

and depends only on the grazing-incidence azimuthal angle γ. Consequently the optimal groove depth does not depend on the period of a grating working in conical diffraction. Consequently when the reflectance of a grating coating material is close to 100% the absolute diffraction efficiency of a grating with properly matched groove depth may be close to the theoretical scalar limit (13) for the chosen groove profile. But again, as is the case for equations (6), (7) and (12), the suitability of equations (14) and (15) for the prediction of the exact positions and values of local and global maxima should be checked by rigorous efficiency calculus.

2.3. Exact electromagnetic theory for very small wavelength-to-period ratios

The theory covered here is necessarily brief because its main parts including peculiarities of diffraction problems at small ratios of λ/p and a more general treatment of the energy conservation law applicable to multilayer absorption gratings have been described at considerable length by Goray & Schmidt (2014). The electromagnetic formulation of diffraction by gratings, which are modelled as infinite periodic structures, can be reduced to a system of Helmholtz equations for the z-components of the electric and magnetic fields in $\mathbf{R}^2$, a finite-dimensional real vector space of dimension two, where the solutions have to be quasiperiodic in the x-direction, subject to radiation conditions in the y-direction, and satisfy certain discontinuity conditions at the interfaces between different materials of the diffraction grating. The actual number of identical or different borders and layers can be large enough, up to a few thousand, for hard X-ray applications. In the case of classical diffraction, when the incident wavevector is orthogonal to the z-direction, the system splits into independent problems for the two basic polarizations as depicted in Fig. 3, whereas in the case of conical diffraction the boundary values of the z-components, as well as their normal and tangential derivatives at the interfaces, are coupled. For gratings in grazing-incidence conical diffraction we refer to linearly polarized incident light whose electric field vector lies in the plane of incidence as the transverse electric (TE) polarization (or p-polarization). Then we define the TM polarization (s-polarization) when the electric field vector lies almost parallel to the plane of the grating. A grating diffracts the incoming plane wave into a finite number of outgoing plane waves considering reflected as well as transmitted modes, *i.e.* orders. The program *PCGrate*® (http://www.pcgrate.com/) computes efficiencies of these orders for an arbitrary number of layers with any boundary profile type.

It is well known that the solutions of the two-dimensional Helmholtz equation with any rigorous numerical code meet with difficulties at small λ/p. While the standard boundary integral equation methods are robust, reliable and efficient, they exhibit poor convergence and loss of accuracy in the long-period range due to numerical contamination in quadrature. Increasing matrix size and enhancing computation precision, as well as applying convergence speed-up techniques, which are successfully explored in short- and mid-period ranges, lead to unreasonably stringent requirements for computing times and storage capacities at long periods and large quantities of layers. In practice, the convergence and accuracy of efficiency computation significantly depend on a proper choice of trial functions, discretization schemes and respective quadrature rules. Usually, one of the collocation methods (method of moments) is used with the distribution of points on a uniform grid. In spite of many research efforts and the increasing power of modern computers, computation of the kernel functions remains a time- and accuracy-critical part of boundary integral equations and other methods for periodic structures, and especially for $\lambda/p \ll 1$. In order to accelerate the convergence of the series representing kernels of the respective operators, different acceleration techniques are applied. While at least one discretization point per wavelength is required to reach efficiency convergence for the usual boundary integral equation methods in X-rays ($\sim$20 is required in the visible range), the modified integral method (MIM) works reliably and fast despite a very small number N of discretization (collocation) points (the main accuracy parameter) per wavelength used in the approach in the X-ray–EUV range. For example, if a period includes $N = 1000$ and $\lambda/p = 1 \times 10^{-7}$ then only 1×10^{-4} points per wavelength is required for the MIM. In the code *PCGrates*, which is based on the MIM, the earlier discovered peculiarity is used in the case of gratings and rough mirrors (*e.g.* Goray & Lubov, 2015) working at very small λ/p: *Introducing known speed-up terms in integral methods produces an adverse numerical effect because of the ensuing uncontrolled growth of coefficients in analytically improved asymptotic estimations* (Goray & Sadov, 2002). In that case, however, the profile depth, the bi-layer thickness (for multilayer gratings) and the radiation wave-

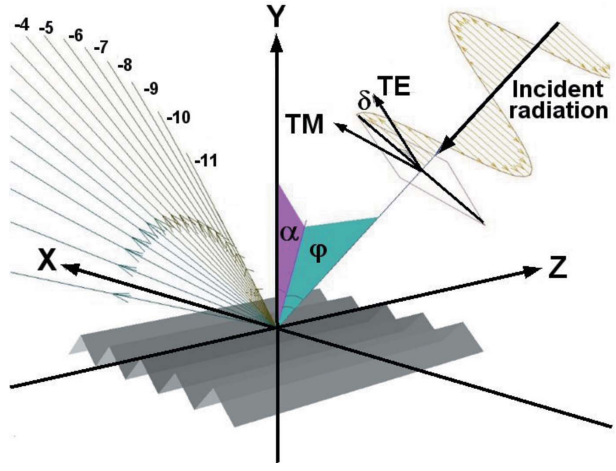

Figure 3
General schematic of diffraction from a periodic structure for a wavefield with two orthogonal field components for an arbitrary angle of incidence and polarization. The TE component of the incident wavefield is considered to be in the plane of incidence, while the TM component is orthogonal to it. The polarization angle δ refers to the inclination angle of the polarization vector with respect to the TE plane for the incident beam. The polar orientation angle φ is connected to the azimuthal grazing incidence angle γ *via* $\varphi = \pi/2 - \gamma$. For the case of conical diffraction γ is used in equation (10) and defined in Fig. 2.

length should be of the same order of magnitude. This is also true for echelles working at any wavelength at high orders.

The MIM transforms the problem of the system of Helmholtz equations into a system of integral operator equations over profile curves. We combine in *PCGrate*® the so-called direct (using the second Green formula) and indirect (using single and double layer potentials) approaches. The solvers only deal with boundary values of the fields and their normal and tangential derivatives. The value of the field in the layers can be found using the boundary data and Green formula. Then, a down–up recursive procedure can be applied using recurrence formulas for initial values of the fields and their derivatives. Thus, both far-zone (amplitudes, phases, efficiencies) and near-zone (absorption, electromagnetic fields and their derivatives) data can be calculated for various groove profiles (including multi-polygonal) and layer (conformal or non-conformal) types, as well as for different substrates and wavefront shapes. In order to account for rigorous random surfaces in the X-ray range we use an infinite beam (plane wave) and assume that the random rough surface length repeats itself for a given large-period grating having a number of random asperities. This classical model implies using infinite grating samples together with intensive Monte Carlo computations (Goray & Lubov, 2015; Goray & Schmidt, 2014).

3. Rigorous efficiency results for perfect laminar gratings

As an example of absolute efficiency predictions using the rigorous method described above we have calculated perfect laminar gratings to check some conclusions derived in §2.2 by using the phenomenological approach. At the here chosen grazing angles of incidence, the results for the TE and for the TM modes are identical. Fig. 4 shows the absolute TE efficiency in the first order of a lamellar Au grating optimized for $\lambda = 0.154$ nm *versus* incidence angle in the in-plane mount for different frequencies: 300 mm^{-1}, 1000 mm^{-1} and 5000 mm^{-1}. According to equation (6) only the first grating could still be used in conditions away from the critical angle operation and thus one expects to find diffraction efficiencies of the order of 10%. The other two gratings with higher groove density will present significantly lower efficiencies. The depths of the grooves have been chosen initially using equation (14) and were then optimized by rigorous efficiency calculus in order to check the suitability of the scalar approach (Born & Wolf, 1980) for the optimization of this parameter. The top-width-to-bottom-width ratio of the lamellar groove profile for all gratings is the same and equal to 4:5. This ratio is applied in all calculations, and the results are only a little different from those for the ratio 1:1. As one can see in Fig. 4, the maximum efficiencies are threefold larger for the 300 mm^{-1} grating in comparison with the 1000 mm^{-1} grating, as predicted by the scalar theory. The rigorously obtained optimal depth $h \simeq 4.8$ nm for the grazing incidence angle $\theta = 0.45^\circ$ differs from the scalar value predicted by equation (14) for the 300 mm^{-1} grating by 20%. The same discrepancy in the depth prediction exists for the 5000 mm^{-1} grating. For the 1000 mm^{-1} grating this discrepancy is even larger with ∼30%. For the 5000 mm^{-1} grating the maximum efficiency is then ninefold smaller in comparison with the maximum efficiency of the 1000 mm^{-1} grating. This is about twofold worse than the scalar theory predicts. As is predicted by equation (14) for frequencies higher than 300 mm^{-1}, the shorter periods provide smaller absolute efficiencies.

The angular dependence of the efficiency of the Au 1220 mm^{-1} perfect laminar grating for various groove depths is shown in Fig. 5 for the TE polarization of the incident radiation at $\lambda = 0.207$ nm. The calculated efficiency is rather low in accordance with the expectation from equation (8) for the present grating, which at wavelengths shorter than 0.6 nm sees the grating to be used beyond the critical angle regime. The exact optimal depth of $h = 4.4$ nm at the grazing incidence angle of ∼0.6° differs for this grating from the scalar value of

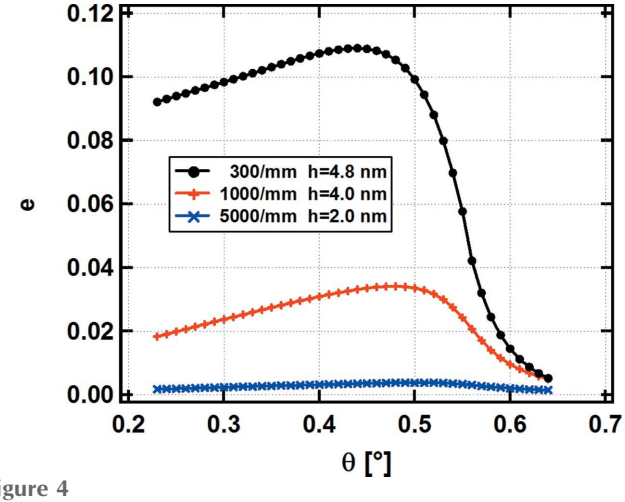

Figure 4
Rigorously calculated efficiency of in-plane laminar Au gratings optimized for $\lambda = 0.154$ nm *versus* incidence angle for various groove densities and rigorously optimized depths.

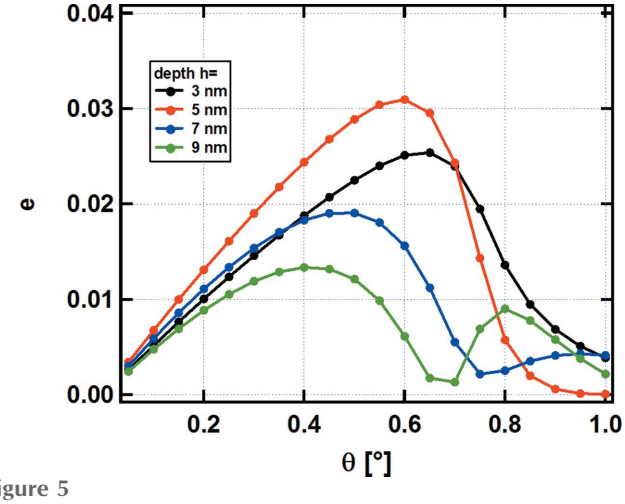

Figure 5
Rigorously calculated efficiency of in-plane laminar Au 1220 mm^{-1} gratings calculated for $\lambda = 0.207$ nm *versus* incidence angle and for various groove depths.

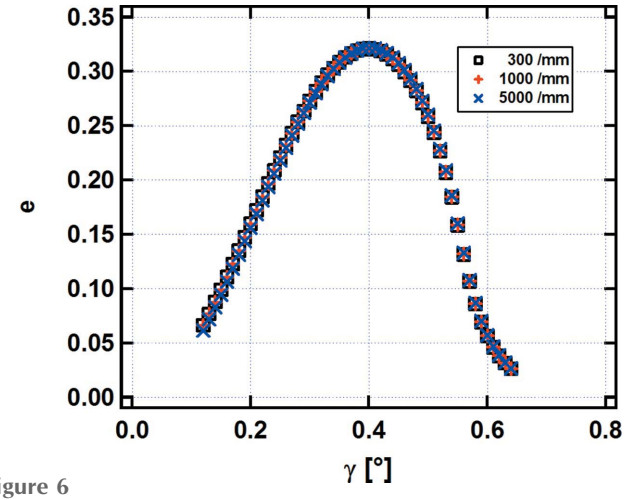

Figure 6
Rigorously calculated efficiency for conical diffraction from laminar Au gratings with a depth of 5 nm optimized for $\lambda = 0.154$ nm *versus* azimuthal incidence for the same groove densities presented in Fig. 4. The critical angle for the Au coating is at 0.56°.

~2.9 nm predicted by equation (14) by more than 30%. The maximal absolute efficiency of more than 3% can be reached in the in-plane orientation for a perfect lamellar groove profile with a top width of 370 nm. As one can see from Fig. 5, the angular-dependent efficiency curves may have two maxima, in accordance with the influence of the optimal depth and reflectance of a grating material under grazing incidence. The scalar approach cannot predict these two maxima.

For conical diffraction mounts, as one can see in Fig. 6, the efficiency maxima and the curve shapes are almost the same for differently dense Au gratings having the same depth, as is predicted by equations (12) and (15). For this conical diffraction efficiency calculus we have used $\alpha = 0°$, $h = 5$ nm and a symmetrical lamellar profile with a top-width-to-bottom-width ratio of 1:1. The maximum absolute efficiency in this condition is three times higher than the maximum efficiency of the 300 mm^{-1} grating in the in-plane configuration as presented in Fig. 5. For smaller grazing incidence angles and higher groove depths the maximum efficiencies in conical diffraction may be even larger and would thus be close to the absolute theoretical limit given in equation (13).

4. Discussion of experimental data

The experimental data for the diffraction efficiency in conical diffraction was compared with a simple prediction by scalar theory in the original publications by Jark & Eichert (2015, 2016). This allowed one to conclude qualitatively that the measured efficiency was relatively high and that it was maximum for the first order approximately at the expected angle of grazing incidence. However, the agreement was not completely satisfying and a successive closer inspection of the grating profile with atomic force microscopy (AFM) gave arguments for this. Indeed the grating profile was found to be distorted compared with the projected profile. In addition, further analysis was made also for the classical orientation. In this case, according to equation (8), the diffraction took place with angles of grazing incidence or diffraction, which are always steeper than the critical angle. This will give rise to significantly transmitted intensity through the coating, which might be partly back-reflected in the valleys. Neither this latter condition nor the profile distortion can be accommodated in a scalar calculation approach. Consequently, in order to make meaningful predictions, the original and the new data were compared with the prediction by use of the required rigorous calculations, which take into account all reflected and transmitted intensities.

4.1. Parameters of the test grating

A comparison between the experimental results and the model expectations is made for the previously reported parameters. The grating was produced in 1990 and has been discussed by Jark (1992). It was projected with a laminar profile with tops of width $\simeq 370$ nm, valleys of width $\simeq 450$ nm and depth $h \simeq 7$ nm. The profile was etched into a polished silicon carbide (SiC) substrate measuring 50 mm × 50 mm × 10 mm on which it covered symmetrically a width of 32 mm and a length of 50 mm. This profile, including also the unetched borders, was then coated with an Au layer of thickness 23 nm. Then in the unetched border sections the roughness statistics for the original substrate should have been replicated in the coating surface. The final real surface profile was measured systematically very recently by AFM. The profile, presented in Fig. 7 for two periods, is a smoothed average over many scan fragments. This profile is the basis for the calculations. The etched profile was found to not be perfectly laminar; instead an additional bump was found in the centre of any profile top. This bump sticks out of an otherwise not flat but concave top. The AFM scans, set for sampling spatial frequencies between 0.5 μm^{-1} and 50 μm^{-1}, also indicate the presence of a significant amount of scratches with widths ranging from 25 nm to about 100 nm. These scratches are present in the unetched border sections and also in the etched structure in the valleys as well as in the tops of the profile. Evidently the etching process did not lead to any smoothing of the scratches. Including the scratches, a relatively large surface roughness with values of the order of

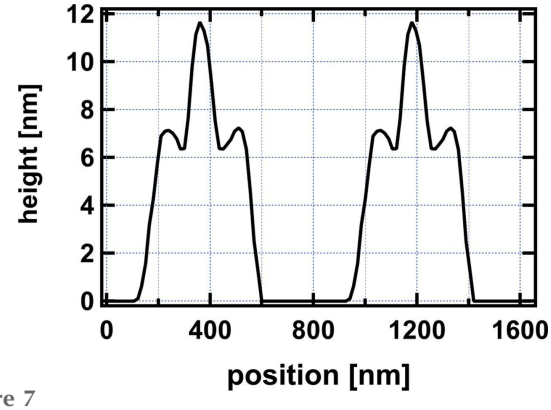

Figure 7
Smoothed averaged profile as used for the simulations, which is obtained from many scans by use of an AFM on the 820 nm-periodic Au groove grating.

1.5 nm r.m.s. is derived in the flat regions. The slope at the sides of the tops of the profiles and of the central bumps, as presented in Fig. 6, is very similar in both positions, ∼80 mrad (or 4.5°). This slope is real and is not an artefact introduced by the shape of the AFM tip.

Since its production several sets of efficiency data have been recorded using the grating at different times, with different groove orientation and in different spectral ranges. According to the criterium for the critical angle operation given in equation (8), this grating can only be used efficiently for in-plane diffraction in the lower-energy soft X-ray range, $E <$ 2 keV, and the diffraction will be rather inefficient at higher photon energies. Alternatively, according to equation (12), in conical diffraction the grating should provide high efficiencies throughout the entire soft X-ray range and even at higher photon energies. The experimental data in the tender X-ray range were then taken in both orientations at higher photon energies, mostly at 4 keV (λ = 0.307 nm) and at 6 keV (λ = 0.21 nm). The entire available data set with significantly different characteristics now presents a very challenging problem to any software for the calculation of grating efficiencies. The principal question is thus whether these data can be predicted with reasonable sample properties for the random surface roughness and accounting for the real groove profile. For the data interpretation it needs to be recognized that the presented data and the AFM scan were obtained at arbitrarily choosen positions. Within the sampling area chosen for the AFM scan of 5 µm × 5 µm the groove depth variation is found to be as large as 1 nm. A similar variation can also be assumed between the different probed areas. So, in principle, for each data set an optimum varying groove depth as well as a groove profile shape could be derived. However, this will not be done here. Instead a single data set is discussed and averaged. Considering the significant variation of the calculated efficiencies with varying groove depth, as shown in Fig. 5, the confidence interval for the calculated efficiency data corresponds for each point to about 20% of the maximum calculated efficiency in each plot. Then the confidence interval is at least two times larger than the presented error bars for the experimental data, which are discussed in the following.

4.2. Efficiency calculus for the real grating and comparison with measurements

The most interesting result found in the previous experiment by Jark & Eichert (2015) for the conical diffraction configuration was the relatively high first-order efficiency of ∼20% each in two symmetrically oriented diffraction peaks for a photon energy of 4 keV. The experimental data up to the third-order diffraction are presented in Fig. 8, where they are compared with the expectations from the rigorous approach taking into account the real grating profile with a valley depth of ∼7 nm, the bump as shown in Fig. 7 and an r.m.s. surface roughness of 1.5 nm r.m.s. The experimental data for the conical diffraction are derived from images taken with a CCD camera mounted behind a transfer lens and a fluorescence screen. The limited sensitivity of the system resulted in an absolute error of $\Delta e = 0.01$ for the efficiency in all orders. The theoretical critical angle for the Au coating is 1.12°.

The calculated angular dependence of the efficiency as well as the absolute values vary rather significantly with the modulation depth next to the central bump on the top surface of the profile. This variation is especially pronounced in the calculations for the zeroth and the third order. In light of this, and considering the related confidence intervals, the overall

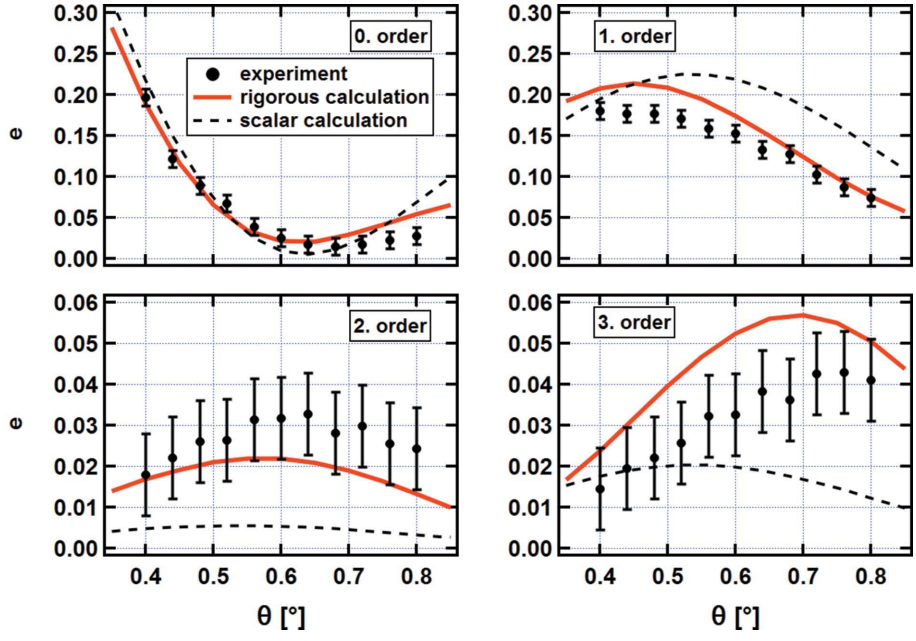

Figure 8
Comparison of the measured grating efficiencies for a photon energy of 4 keV (λ = 0.307 nm) for different orders (zeroth to third) in the conical diffraction scheme as measured by Jark & Eichert (2015) with the calculations using the rigorous approach accounting for the real grating profile (solid line). The prediction by the scalar theory is shown by the dashed line.

agreement of the calculations with the experimental data even for higher diffraction orders is rather satisfying.

Practically speaking it is very promising that the efficiency for the technically more relevant first order can be predicted with rather small error. This applies when one considers the real and not ideal groove profile. Even though the surface roughness is rather high at 1.5 nm r.m.s., this parameter does not affect the first-order efficiency very much. In fact, the expected efficiency for zero roughness is only slightly larger at about 23%.

At this point we ask whether the simple scalar approach can be used for making some predictions? Thus in Fig. 8 we also present as dashed lines the predictions with the scalar theory, in this case for an ideal laminar profile with a top-width-to-bottom-width ratio of 0.45:0.55. On the one hand, the predictions using the rigorous approach show relatively little variation for the first-order efficiency with variation of the bump in the real profile. On the other hand, the prediction with the simple scalar model for this more relevant order is significantly different compared with the rigorous calculations. Consequently the scalar approach provides rather unreliable predictions, which is even more the case for higher orders and especially towards steeper angles of incidence. As far as the angular dependences are concerned, the scalar approach only succeeds in indicating the position for minimum efficiency into the zeroth diffraction order, while it cannot predict any other extreme performance (minimum/maximum).

The angular dependences of the diffraction efficiencies in the case of the rigorous calculation model in Fig. 8 are obtained for a groove depth of ~7 nm. This depth will also affect the diffraction efficiency in the in-plane case. As far as the zeroth order in this grating orientation is concerned, one can easily measure it in a θ–2θ scan, *i.e.* in a specular reflectivity scan. The related spectrum, which is not presented here, shows a periodic oscillation introduced by interference in the coating thickness (see, for example, Born & Wolf, 1980), and an additional weak zeroth-order diffraction peak at an angle of grazing incidence of 1.5° (for λ = 0.31 nm), which is significantly above the theoretical critical angle of 1.12°. This peak is predicted by the rigorous approach, which considers all reflected and transmitted waves and their deformations due to shadowing, for the indicated groove depth of 7 nm.

The measured data for the first-order in-plane diffraction at a larger photon energy of 6 keV (λ = 0.207 nm) are presented in Fig. 9. The experimental error Δe in this case of operation beyond the critical angle limit according to equation (8) and thus of rather small efficiency is constant, corresponding to 10% of the measured signal at the maximum. The simulation confirms the small diffraction efficiency for the profile presented in Fig. 7 and for an r.m.s. surface roughness of 1.5 nm. The angular dependence is slightly different. However, it is found that the absolute value of the efficiency as well as the angular dependence undergo significant changes upon variation of any of the important parameters, *i.e.* groove depth, slope in the sides of the top surfaces and the bumps, and r.m.s. roughness. For the considered grating the most critical parameters are the groove depth and the r.m.s. roughness. In

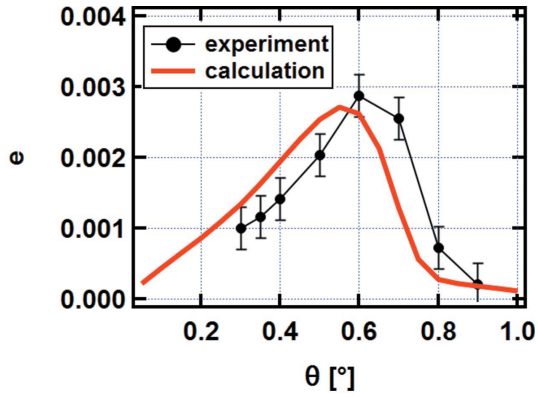

Figure 9
Comparison between the measured angular dependent efficiency for the first order of the laminar Au 1220 mm^{-1} grating for λ = 0.207 nm and the rigorous simulation for the real profile and an r.m.s. roughness of 1.5 nm in in-plane diffraction.

fact Fig. 5 has already shown that the predicted efficiency curves undergo significant changes with variation of the groove depth for zero roughness. Thus achieving a better agreement was not attempted. In this case, without roughness, the first-order efficiency is predicted to be about 0.75%, and thus the relatively large roughness of 1.5 nm r.m.s. reduced it threefold.

At this point it becomes interesting to see whether, and how well, the rigorous approach can predict, for the real groove profile, the in-plane diffraction under more favourable conditions as far as operation away from the critical angle is concerned. According to equations (8) and (9) these conditions will be found for longer wavelengths, *i.e.* for smaller photon energies. The grating was a test structure for verifying the suitability of the laminar profile in a heat-resistant substrate (SiC) for a soft X-ray monochromator to be operated at high heat load from an undulator synchrotron radiation source, as discussed by Jark (1992). The proposed driving scheme for the monochromator was the fixed-focus SX700 scheme introduced by Petersen (1982), in which the virtual vertical source is kept at a fixed distance upstream of the grating by simply running it with $\sin\phi/\sin\theta$ = constant = 2.25. The grating profile and this latter ratio will allow us to estimate its efficiency. This operation will take place away from the critical angle operation. Then at the correspondingly operated rather small angles of grazing incidence the shadow effect in the valleys will mean that the valleys hardly contribute in the diffraction. So the structure could be looked upon as a simple binary grating with absorbing valleys. For such a structure the efficiency in first order in the scalar model according to Born & Wolf (1980) would be expected to be about 10% of the related reflectivity of the coating. Initially the grating efficiency was tested by Jark *et al.* (1990) for the projected operation range with photon energies between 100 eV and 800 eV. In fact, the reported data, as discussed by Jark *et al.* (1990) and Jark (1992), show that the experimentally observed efficiency was roughly 10% of the reflectivity of a gold coating at the same angles of grazing incidence. When the real profile and the surface roughness are now considered in

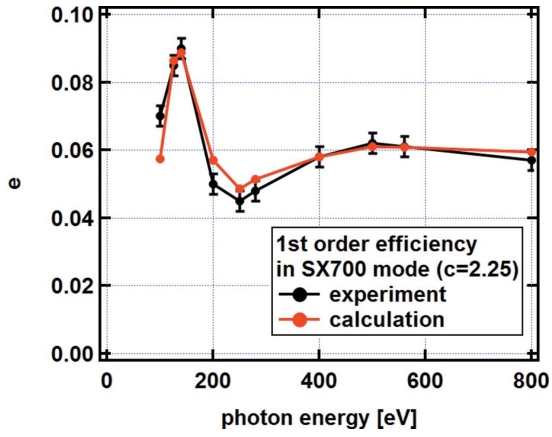

Figure 10
Comparison between experimentally measured first-order efficiencies by Jark (1992) and those calculated rigorously with the real groove profile of the 1220 mm^{-1} laminar grating *versus* photon energy in in-plane diffraction. The grating was operated in the fixed-focus condition, with constant ratio $\sin\phi/\sin\theta = 2.25$.

the simulations, then, as shown in Fig. 10, the predicted efficiencies almost agree with the observed efficiencies for the SX700 operation mode. In this case the error in the measured efficiency Δe is constant and corresponds to 3% of the measured signal in the maximum.

Another test was run at a photon energy of 1400 eV (λ = 0.89 nm) by Di Fonzo *et al.* (1991). In this case, according to equation (8), the first-order diffraction takes place in the vicinity of the critical angle operation, while the second-order diffraction takes place beyond this critical angle limit. The latter related diffraction is thus expected to be very inefficient. Note that in any case the second-order diffraction from a laminar (binary) grating should be very small (see, for example, Hutley, 1982). Even under these very particular conditions, as is evident from Fig. 11, the rigorous calculations predict the angular dependence of the efficiency and its absolute expectedly small values, which were measured by

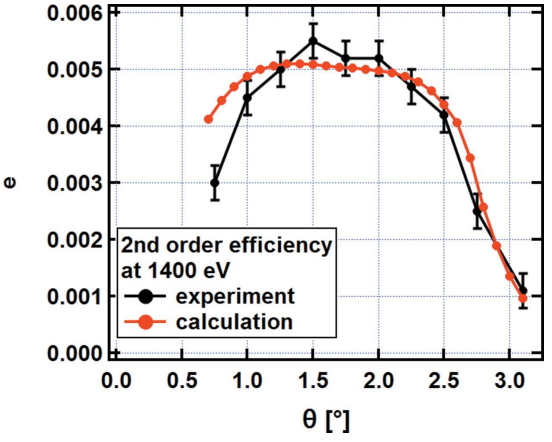

Figure 11
Comparison between the experimentally measured 1220 mm^{-1} laminar grating efficiencies for the second order *versus* angle of grazing incidence in in-plane diffraction for a photon energy of 1400 eV by Di Fonzo *et al.* (1991) and those calculated rigorously with the real groove profile.

Di Fonzo *et al.* (1991). In this case of measured small signals the error Δe corresponds to 5% of the measured signal in the maximum.

5. Summary

This contribution shows that by the use of rigorous calculations taking into account the real grating profile of a diffraction grating the expected performance of the grating can now be predicted rather reliably in the entire soft X-ray range including the tender X-rays. This applies in the present case for both possible grating orientations with respect to the incident beam, *i.e.* when the diffraction is rather inefficient in in-plane mounts as well as when the diffraction is found to be rather efficient for conical diffraction mounts. A relatively large surface roughness of the order of 1.5 nm r.m.s. was found to have little effect in the latter case on the first-order efficiency in the prediction as well as in the measured data. It is shown that the scalar approach for the efficiency calculation will fail for this purpose. The relatively high diffraction efficiency for the present reflection grating in the conical diffraction configuration throughout the tender X-ray range now also allows us to consider gratings as optical devices to be used in instruments for this spectral range. The present grating with laminar profile turns out to provide interesting symmetric and efficient beam-splitting properties, as predicted by Goray (2008). In gratings with other profiles, the diffraction with high efficiency into a single order could be favoured and such devices could then find applications in monochromators. Jark (2016) showed that unusual tuning ranges, *e.g.* 600–6 keV, could be scanned with just a single grating. Scanning in this range presently requires the employment of several rather different dispersing elements. The application of the conical diffraction configuration has already been discussed for lower-energy soft X-rays in space astronomy and in free-electron-laser research. In the first case it is an efficient means for the monochromatization of weak soft X-ray signals (see, for example, Werner, 1977; Cash, 1991; Goray & Egorov, 2016), while in the latter case at strong sources the efficiency becomes an argument when two diffracting elements are used, as proposed by Poletto (2004), in order to minimize the pulse lengthening, which is inherent in the diffraction from single reflection gratings. In both cases the rigorous calculation approach described here holds the capability to become a powerful tool for the optimization of the profile in already projected spectral ranges with smaller photon energy, but also when larger photon energies are considered.

Acknowledgements

The authors gratefully acknowledge Dr P. Parisse of Elettra Sincrotrone Trieste for providing the AFM scans, and Dr G. Schmidt from WIAS for providing valuable information. Dr B. Nelles from DIOS GmbH and Dr H. Kierey and Dr B. Kleemann from Zeiss are acknowledged for commenting on the origin of the bumps on the grating structure. The yet unpublished experimental data were obtained

during in-house research beam time at the X-ray fluorescence beamline 10.1L at Elettra.

Funding information

Funding for this research was provided by: Ministry of Education and Science of the Russian Federation, Russian Foundation for Basic Research (RFBR) (grant No. 17-02-00362, 16-29-11697 to Leonid Goray); National Basic Research Program (Program 973) (grant No. 2014AA014402).

References

Attwood, D. (1999). *Soft X-rays and Extreme Ultraviolet Radiation: Principles and Applications*, ch. 8. Cambridge University Press.

Born, M. & Wolf, E. (1980). *Principles of Optics*, ch. 8.6. New York: Macmillan.

Cash, W. C. (1991). *Appl. Opt.* **30**, 1749–1759.

Cash, W. & Kohnert, R. (1982). *Appl. Opt.* **21**, 17–18.

Choueikani, F., Lagarde, B., Delmotte, F., Krumrey, M., Bridou, F., Thomasset, M., Meltchakov, E. & Polack, F. (2014). *Opt. Lett.* **39**, 2141–2144.

Di Fonzo, S., Jark, W., Müller, B. R., Schäfers, F. & Puik, E. J. (1991). *BESSY Annual Report 1991*, pp. 494–496. BESSY, Berlin, Germany.

Gorai, L. I. (2005). *Bull. Russ. Acad. Sci. Phys.* **69**, 231–236.

Goray, L. I. (2008). *J. Synch. Investig.* **2**, 796–800.

Goray, L. I. & Egorov, A. Yu. (2016). *Appl. Phys. Lett.* **109**, 103502.

Goray, L. & Lubov, M. (2015). *Opt. Express*, **23**, 10703–10713.

Goray, L. I. & Sadov, S. Yu. (2002). *OSA Trends Opt. Photon. Ser.* **75**, 365–378.

Goray, L. I. & Schmidt, G. (2014). *Boundary Integral Equation Methods for Conical Diffraction and Short Waves*, in *Gratings: Theory and Numerical Applications*, 2nd rev. ed., edited by E. Popov. Presses Universitaires de Provence, AMU.

Greig, J. H. & Ferguson, W. F. C. (1950). *J. Opt. Soc. Am.* **40**, 504–505.

Henke, B. L., Gullikson, E. M. & Davis, J. C. (1993). *At. Data Nucl. Data Tables*, **54**, 181–342.

Hutley, M. (1982). *Diffraction Gratings (Techniques of Physics)*. New York: Academic Press.

Ishino, M., Heimann, P. A., Sasai, H., Hatayama, M., Takenaka, H., Sano, K., Gullikson, E. M. & Koike, M. (2006). *Appl. Opt.* **45**, 6741–6745.

James, R. W. (1967). *The Optical Principles of the Diffraction of X-rays*. Cornell University Press.

Jark, W. (1992). *Rev. Sci. Instrum.* **63**, 1241–1246.

Jark, W. (2016). *J. Synchrotron Rad.* **23**, 187–195.

Jark, W., Blessing, C. & Heidemann, K. F. (1990). *HASYLAB Annual Report 1990*, pp. 579–580. HASYLAB, Germany.

Jark, W. & Eichert, D. (2015). *Opt. Express*, **23**, 22753–22764.

Jark, W. & Eichert, D. (2016). *J. Synchrotron Rad.* **23**, 91–97.

Lukirskii, A. P., Savinov, E. P. & Shepelev, Y. P. (1963). *Opt. Spectrosc.* **15**, 290–293.

McNulty, I., Feng, Y., Frigo, S. P. & Mooney, T. M. (1997). *Proc. SPIE*, **3150**, 195–204.

Matsushita, T. & Hashizume, H. (1983). *X-ray Monochromators*, in *Handbook of Synchrotron Radiation*, Vol. 1b, edited by E. E. Koch, pp. 261–314. Amsterdam: North Holland.

Maystre, D., Neviere, M. & Petit, R. (1980). *Experimental Verifications and Applications of the Theory*, in *Electromagnetic Theory of Gratings*, edited by R. Petit. Berlin: Springer.

Maystre, D. & Petit, R. (1976). *Nouv. Rev. Opt.* **7**, 165–180.

Neviere, M. & Flamand, J. (1980). *Nucl. Instrum. Methods*, **172**, 273–279.

Petersen, H. (1982). *Opt. Commun.* **40**, 402–406.

Petersen, H. (1986). *Nucl. Instrum. Methods Phys. Res. A*, **246**, 260–263.

Poletto, L. (2004). *Appl. Phys. B*, **78**, 1013–1016.

Senf, F., Bijkerk, F., Eggenstein, F., Gwalt, G., Huang, Q., Kruijs, R., Kutz, O., Lemke, S., Louis, E., Mertin, M., Packe, I., Rudolph, I., Schäfers, F., Siewert, F., Sokolov, A., Sturm, J. M., Waberski, C., Wang, Z., Wolf, J., Zeschke, T. & Erko, A. (2016). *Opt. Express*, **24**, 13220.

Vidal, B., Vincent, P., Dhez, P. & Neviere, M. (1985). *Proc. SPIE*, **0563**, 142–149.

Vincent, P., Nevière, M. & Maystre, D. (1979). *Appl. Opt.* **18**, 1780–1783.

Voronov, D. L., Goray, L. I., Warwick, T., Yashchuk, V. V. & Padmore, H. A. (2015). *Opt. Express*, **23**, 4771–4790.

Voronov, D. L., Salmassi, F., Meyer-Ilse, J., Gullikson, E. M., Warwick, T. & Padmore, H. A. (2016). *Opt. Express*, **24**, 11334–11344.

Werner, W. (1977). *Appl. Opt.* **16**, 2078–2080.